

Preparation and properties of high-performance polyimide copolymer fibers derived from 5-amino-2-(2-hydroxy-4-aminobenzene)-benzoxazole

Xuemin Dai^{ab} (代学民), Feng Bao^b (鲍峰), Yongfeng Men^a and Xuepeng Qiu^{b*} (邱雪鹏)

^a State Key Laboratory of Polymer Physics and Chemistry, Changchun Institute of Applied Chemistry, Chinese Academy of Sciences, Changchun 130022, P. R. China. (中国科学院长春应用化学研究所)

^b Polymer Composites Engineering Laboratory, Changchun Institute of Applied Chemistry, Chinese Academy of Sciences, Changchun 130022, P. R. China.

* Corresponding author Tel: +86 431 85262095. Fax: +86 431 85262095

E-mail address: xp_q@ciac.ac.cn

Abstract

A series of high-performance polyimide copolymer (co-PI) fibers containing phenylenebenzoxazole moiety with one hydroxyl group are synthesized based on the copolymerization of 3,3',4,4'-biphenyl tetracarboxylic dianhydride (BPDA) with two diamine monomers, namely, *p*-phenylenediamine (*p*-PDA) and 5-amino-2-(2-hydroxy-4-aminobenzene)-benzoxazole (*p*-mHBOA), through a two-step method. Influences of the *p*-mHBOA moieties on the thermal stability, crystal structure, crystal orientation, microvoid morphology, and mechanical properties are systemically investigated. The glass transition temperatures (T_{gs}) of co-PI fibers are in the range of 290–325 °C. The prepared fibers show excellent thermal stabilities, and their $T_{5\%}$ is within 528–542 °C in air. Two-dimensional wide-angle X-ray diffraction spectra indicate that homo-PI and co-PI fibers present a regularly arranged polymer chains along the fiber axial direction. Moreover, the ordered molecular packing along the transversal direction of fibers is destroyed by the copolymerization. Small-angle X-ray scattering results show that co-PI fibers with optimal mechanical properties exhibit the shortest average length (L) and the smallest radius (\bar{r}) of microvoids. When the *p*-mHBOA/*p*-PDA molar ratio is 5/5, the fracture strength and initial modulus can reach approximately 30.31 cN/dtex (4.40 GPa) and 894.88 cN/dtex (129.8 GPa), respectively.

Keywords:

Polyimide fiber; Phenylenebenzoxazole; Hydrogen bonding

1. INTRODUCTION

Aromatic polyimide (PI) fibers are well-known high performance fibers that exhibit excellent physical and chemical properties: thermal stability [1, 2], solvent resistance [3, 4], electrical insulation [5, 6] and radiation resistance [7, 8]. Given these properties, aromatic PI fibers have been widely applied in high-temperature dedusting, special protection, aerospace industries and composite material. Ideal high-performance fibers should possess high tensile strength and initial modulus. However, the mechanical properties of commercial PI fibers including P84[®], Suplon[®] and Yilun[®] are inadequate to satisfy the requirements of high-technology products. The main problem is the poor processability of the PI fibers.

Definitely, the spinning process and chemical structure influence the mechanical properties of the PI fibers. Considerable efforts have been exerted in the spinning process, such as spinning solution, spinning technology and post-treatment conditions. Moreover, much attention has been given to the modification of the chemical structure of the PI fibers. Copolymerization of additional diamines or

dianhydrides into the polymer backbone is the most effective approach to improve the mechanical properties of PI fibers. Particularly, some types of rigid aromatic heterocyclic diamines, such as 2,5-bis(4-aminophenyl)-pyrimidine (2,5-PMR), 2-(4-aminophenyl)-6-amino-4(3H)-quinazolinone (AAQ), 2,6-(4,4'-diaminosiphenyl) benzo [1,2-d; 5,4-d'] bisoxazole (PBOA) and 2-(4-aminophenyl)-5-aminobenzimidazole (BIA) have been introduced into the PI backbones, and they are proven effective in improving the mechanical properties of the fibers. For example, Wu *et al.* [9] prepared a new type of co-PI fibers by introducing AAQ into the rigid backbones of 3,3',4,4'-biphenyl tetracarboxylic dianhydride (BPDA) and *p*-phenylenediamine (*p*-PDA). The tensile strength and initial modulus of the co-PI fiber reached to 2.8 GPa and 115 GPa, respectively, by adjusting the percentage of the AAQ content. Zhang and co-workers [10] discovered that increasing the BIA moiety in the BPDA/BOA backbone remarkably improves the mechanical properties, i.e. tensile strength and initial modulus increase from 1.29 GPa to 1.74 GPa and from 40.1 GPa to 74.4 GPa, respectively.

Intermolecular hydrogen bonding (H-bonding) is crucial in improving the mechanical properties of rigid polymer fibers, such as Kevlar [11,12], Armos [13] and M5 [14,15]. Currently, rigid units bearing functional groups including benzimidazole [16, 17] and quinazolinone [18,19] in the backbone of PI fibers have been extensively investigated. The –NH– group of the benzimidazole or quinazolinone units can form H-bonding with the oxygen atom of the carbonyl group of the cyclic imide. Previous reports [20-22] indicated that the introduction of hydroxyl groups can also form H-bonding among the rigid polymer chains and remarkably enhance the mechanical properties of fibers. Nonetheless, the hydroxyl group in the molecular chains of PI fibers has not been reported.

In the present study, a novel hydroxyl-containing phenylenebenzoxazole diamine monomer, that is, 5-amino-2-(2-hydroxy-4-aminobenzene)-benzoxazole (*p*-mHBOA) depicted in Scheme 1, is designed and synthesized. Subsequently, a series of co-PI fibers are fabricated via a two-step method based on the copolymerization of BPDA, *p*-PDA and *p*-mHBOA. Homo-BPDA/*p*-PDA and homo-BPDA/*p*-mHBOA PI fibers also have been prepared for comparison with co-PI fibers. The effects of the *p*-mHBOA moieties on the microstructure and the thermal and mechanical properties of co-PI fibers are systematically investigated.

2. EXPERIMENTAL

2.1 Materials

N,N-dimethylacetamide (DMAc) was purchased from Xilong Chemical Co. Ltd. (Guangdong, China) and used directly. 5-amino-2-(2-hydroxy-4-aminobenzene)-benzoxazole (*p*-mHBOA) was synthesized in our laboratory. 3,3',4,4'-Biphenyl tetracarboxylic dianhydride (BPDA) and *p*-phenylenediamine (*p*-PDA) were purchased from Changzhou Sunlight Medical Raw Material Co. Ltd. (Jiangsu, China) and purified by sublimation before use.

2.2 Fabrication of PAA fibers

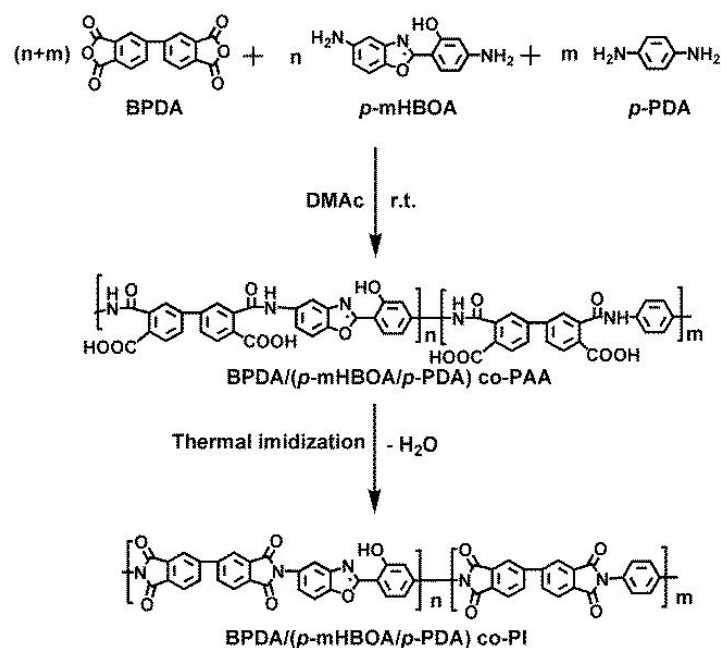
The PAA solutions were firstly synthesized by dissolving *p*-mHBOA/*p*-PDA in DMAc under a nitrogen atmosphere. Afterwards, an equimolar amount of BPDA was gradually added. The reaction was carried out at 25 °C for 48 h. The viscous PAA solutions with different *p*-mHBOA/*p*-PDA molar ratios (0/10, 1/9, 3/7, 5/5, 7/3, 9/1 and 10/0) were obtained.

The PAA fibers were produced through dry-jet wet spinning process. The above-mentioned PAA solutions were filtered and degassed at room temperature. These solutions were subsequently extruded

through a spinneret with 50 orifices (each with 0.12 mm in diameter) through a short air gap into a H₂O/DMAc coagulation bath with a draft ratio of 3.0. The obtained fibers were dried at 50 °C for 12 h.

2.3 Fabrication of PI fibers

The above-mentioned PAA fibers were converted to PI fibers by successive heating from room temperature to 380 °C at a heating rate of 7 °C /min under vacuum, and maintained at 380 °C for 30 min. The imidized fibers were drawn at different ratios to obtain the final PI fibers. Scheme 1 shows the synthetic process and chemical structure of the co-PI fibers.



Scheme 1. Two-step procedure for the preparation of homo-PI and co-PI fibers ($n/m = 0/10, 1/9, 3/7, 5/5, 7/3, 9/1$ and $10/0$).

2.4 Characterization

The inherent viscosities (η_{inh}) of PAA solutions were measured with an Ubbelohde viscometer at a concentration of 0.5 g·dL⁻¹ in DMAc at 30 °C.

Fourier transform infrared (FTIR) spectra were obtained with a VERTEX 70 spectrometer in the range of 4000–400 cm⁻¹.

Dynamic mechanical thermal analysis (DMA) was carried out with the Rheometric scientific DMTA-V at a heating rate of 10 °C/min and a load frequency of 1 Hz in the fiber tension geometry under nitrogen atmosphere. The glass transition temperature (T_g) was regarded as the peak temperature in the $\tan \delta$ curve.

Thermo-gravimetric analysis (TGA) was performed with a TA-Q50 instrument in dynamic nitrogen and air environments at a heating rate of 10 °C/min.

Two-dimensional wide-angle X-ray diffraction (2D WAXD) measurements for PI fibers were performed on a Nano-inXider system of Xenocs France equipped with a semiconductor detector (Pilatus 100K, Dectris, Swiss) attached to a multilayer focused Cu $K\alpha$ X-ray source (GeniX^{3D} Cu ULD, Xenocs SA, France).

Two-dimensional small-angle X-ray scattering (2D SAXS) experiments were performed using a GeniX^{3D} Cu ULD (Xenocs SA, France) with Cu $K\alpha$ radiation (wavelength, $\lambda=0.154$ nm). The generator was operated at 40 kV and 650 μ A. 2D SAXS patterns were obtained using a Pilatus 100K

detector (Dectris, Swiss, 487 pixels × 198 pixels, pixel size = 172 μm).

The mechanical properties were measured with Textechno FAVIMAT instrument, with a gauge length of 20 mm and an extension rate of 5 mm/min. The initial modulus was taken as the slope of the stress-strain curve between 0.2% and 0.4% elongation, and at least 10 filaments were evaluated for each type of fibers.

3. RESULTS AND DISCUSSION

3.1 Synthesis of PAA solutions

A series of PAA solutions are prepared using different molar ratios of *p*-mHBOA/*p*-PDA with BPDA. Table 1 shows that the inherent viscosities (η_{inh}) of PAA solutions are 2.78, 2.53, 2.34, 2.26, 2.21, 2.10 and 1.97 dL/g, which correspond to the molar ratios of *p*-mHBOA/*p*-PDA, i.e. 0/10, 1/9, 3/7, 5/5, 7/3, 9/1 and 10/0, respectively. Evidently, η_{inh} decreases with the increased *p*-mHBOA content, which may be attributed to the poor electron-donating ability of the amino group in *p*-mHBOA monomer.

Table 1 Inherent viscosity of the PAA solutions of corresponding PI fibers.

Sample	<i>p</i> -mHBOA/ <i>p</i> -PDA (molar ratio)	η_{inh} (dL/g)
homo-PI-0	0/10	2.78
co-PI-1	1/9	2.53
co-PI-2	3/7	2.34
co-PI-3	5/5	2.26
co-PI-4	7/3	2.21
co-PI-5	9/1	2.10
homo-PI-0'	10/0	1.97

3.2 Structure characterization of the prepared PI fibers

The chemical structure of the PI fibers is identified by ART-IR spectra, as shown in Fig. 1. All the PI fibers display four characteristic absorption peaks at approximately 1772, 1701, 733 and 1353 cm⁻¹, which are attributed to the C=O asymmetrical stretching, symmetrical stretching and bending, and C–N stretching of the cyclic imide, respectively. The characteristic absorption peak near 1655 cm⁻¹ for the C=O asymmetrical stretching of the amide group disappears, thereby indicating a high imidization degree of resultant PI fibers. Moreover, two apparent absorption bands are centered at 1582 cm⁻¹ and 1256 cm⁻¹, which correspond to benzoxazole C=N– asymmetric stretching and benzoxazole Ar–O–C asymmetric stretching. Their intensities increase with the content of *p*-mHBOA monomer in fibers. Additionally, the characteristic absorption peak at approximately 3400 cm⁻¹ for –OH stretching cannot be detected due to the formation of intramolecular H-bonding or/and intermolecular H-bonding (Fig. 2), but the apparent absorption band at about 1195 cm⁻¹ for Ar–OH stretching can be observed in co-PI fibers. This result implies that *p*-mHBOA moiety is successfully incorporated into the backbones of co-PI fibers.

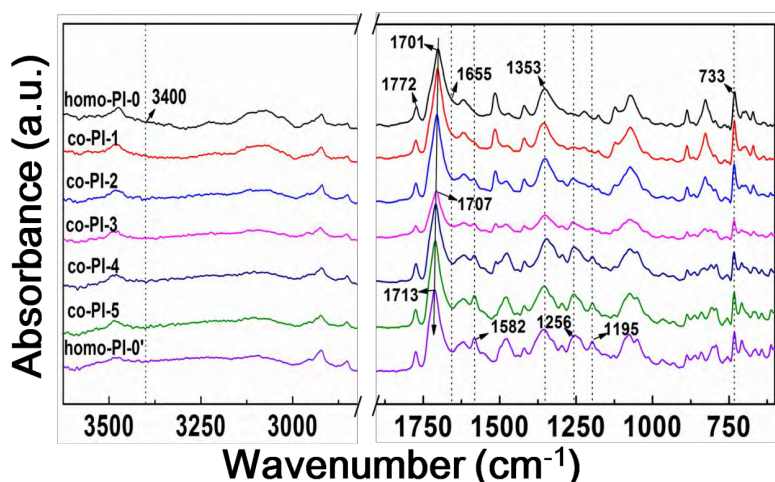


Fig. 1. FTIR spectra of the prepared PI fibers with different diamine monomer molar ratios.

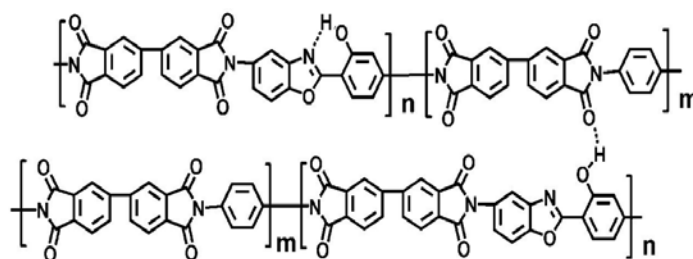


Fig. 2. Inter-/intramolecular H-bonding in co-PI structure.

3.3 Glass transition temperature and thermal stability

The glass transition temperature (T_g) is determined by DMA as shown in Fig. 3. Detailed peak temperatures in $\tan\delta$ curves are listed in Table 3. Their T_g s are 325 °C, 306 °C, 297 °C, 295 °C, 290 °C, 298 °C and 307 °C, which correspond to the *p*-mHBOA/*p*-PDA molar ratios of 0/10, 1/9, 3/7, 5/5, 7/3, 9/1 and 10/0, respectively. Although the addition of *p*-mHBOA is beneficial to increase the intermolecular interactions, the regularity of the molecular chains becomes lower to facilitate the movement of the molecular segments. Nevertheless, continuing to increase the content of *p*-mHBOA causes an increase in the regularity of the molecular chains, and forms stronger inter-/intramolecular H-bonding interaction which can hinder the segmental motion of polymer chains to some extent.

The thermal stability of fibers is investigated by TGA as shown in Fig. 4. The temperature at 5% weight loss ($T_{5\%}$) and 10% weight loss ($T_{10\%}$) under nitrogen and air atmospheres, and the percentage of residue at 850 °C in nitrogen atmosphere are summarized in Table 3. The $T_{5\%}$ values of the fibers are in the range of 557 °C–593 °C and 528 °C–542 °C in nitrogen and air atmosphere, respectively. The $T_{10\%}$ values are in the range of 580 °C–607 °C and 547 °C–567 °C in nitrogen and air atmospheres, respectively. Moreover, the char yields at 850 °C under nitrogen atmosphere are within 60.6 wt% – 63.3 wt%. The OH groups in *p*-mHBOA are more readily oxidized than those in BPDA/*p*-PDA parts, but the benzoxazole moiety possesses excellent thermal and thermo-oxidative stabilities. Although the $T_{5\%}$ and $T_{10\%}$ values of the fibers under both air and nitrogen atmospheres slightly decrease with the incorporation of the *p*-mHBOA, the copolymer fibers maintain their excellent thermal and thermo-oxidative stabilities.

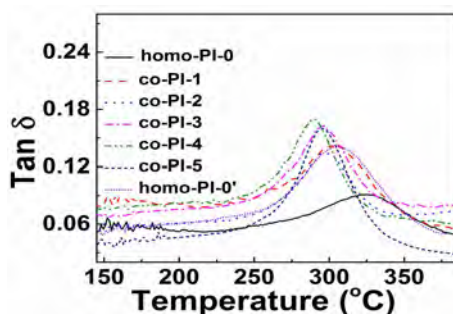


Fig. 3. DMA curves of the prepared fibers with *p*-mHBOA content for PI fibers.

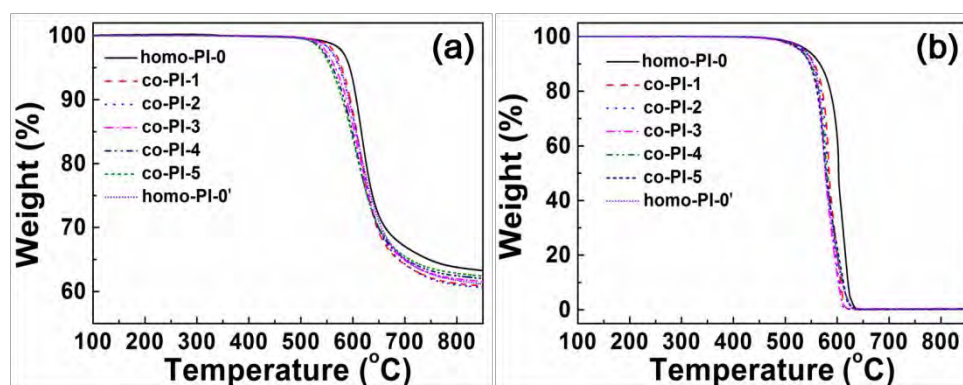


Fig. 4. TGA of the prepared fibers with different diamine monomer molar ratios in (a) N₂ and (b) air atmospheres.

Table 3. Thermal properties of the prepared PI fibers with different diamine monomer molar ratios.

Sample	T_g (°C) ^a	Weight loss (°C)				Char yield (%) ^b
		In air		In N ₂		
		$T_{5\%}$	$T_{10\%}$	$T_{5\%}$	$T_{10\%}$	
homo-PI-0	325	542	567	593	607	63.3
co-PI-1	306	536	556	578	595	60.9
co-PI-2	297	534	554	573	593	60.6
co-PI-3	295	528	548	566	587	61.6
co-PI-4	290	530	549	561	583	62.0
co-PI-5	298	529	547	557	580	62.4
homo-PI-0'	307	538	554	575	593	61.2

^a Peak temperature of tan δ measured by DMA at a heating rate of 10 °C/min.

^b Percentage of carbon residue at 850 °C in nitrogen atmosphere.

3.4 Crystal structure and molecular orientation

Crystallinity and orientation degree play important roles in the mechanical properties of polymeric fibers. Fig. 5(a–g) displays the 2D WAXD patterns of the fibers with different molar

ratios. Several clear diffraction streaks can also be observed in Fig. 5(a–g) along the meridian direction, and they reveal a regularly arranged polymer chains along the fiber axial direction. In the equator direction, the 2D WAXD patterns of two homo-PI fibers in Fig. 5a and 5g show a few clear diffraction streaks, which demonstrate ordered molecular packing along the transversal direction of the fibers. Noticeable changes in the patterns can be observed in Fig. 5(b–f) after incorporating *p*-mHBOA. The equatorial diffraction streaks gradually become further diffuse into the co-PI-4 fiber with *p*-mHBOA/*p*-PDA molar ratio of 7/3, which demonstrates a reduced ordered packing along the transversal direction of the fibers. However, the equatorial diffraction streaks of the co-PI-5 fiber with *p*-mHBOA/*p*-PDA molar ratio of 9/1 are clear, which indicate an increase in the lateral packing order along the transversal direction of fibers. Moreover, these prepared PI fibers shows a typical crystallization structure, which is different from those fibers spun from liquid crystalline states, such as lyotropic aramids, lyotropic aromatic heterocyclic polymers and the family of thermotropic aromatic copolyesters.

To investigate the crystalline structure in PI fibers, 1D WAXD patterns along the equator and meridian directions are obtained (Fig. 6a and 6b) by integrating their 2D WAXD patterns. Along the equator direction, three diffraction peaks are observed at $2\theta = 13.1^\circ$, 18.2° and 25.5° for the homo-PI-0 fiber in Fig. 6a. These diffraction peaks gradually broaden or disappear with the increase in *p*-mHBOA content until 70%. This result indicates a decrease in the lateral packing order from the random distribution of BPDA/*p*-PDA and BPDA/*p*-mHBOA units in polymer chains. When the *p*-mHBOA content increases to 90%, new diffraction peaks appeared. The homo-PI-0' fiber, there are four sharp diffraction peaks at $2\theta = 14.2^\circ$, 24.0° , 26.0° and 28.5° in the equator direction. These peaks indicate the formation of a new ordered packing along the transversal direction of fibers.

In the meridian direction, as depicted in Fig. 6b, several diffraction peaks are observed for each fiber, and they suggest a regular arrangement of the polymer chains along the fiber axial direction. The diffraction peak positions of two homo-PI fibers are completely different, which reveals the difference in the crystal structures of the two polymer fibers. The diffraction peaks with relatively strong intensity for each fiber are also observed at $2\theta = 11.2^\circ$, 11.4° , 11.7° , 12.0° , 12.2° , 12.4° and 12.6° , which correspond to homo-PI-0, co-PI-1, co-PI-2, co-PI-3, co-PI-4, co-PI-5 and homo-PI-0' fibers, respectively. The *p*-mHBOA incorporation causes the diffraction peaks to move to a high diffraction angle, which indicates a decrease in *d*-spacing due to the asymmetric structure of *p*-mHBOA moiety and formation of strong inter-/intramolecular H-bonding. In addition, a few peaks disappear for co-PI fibers compared with the homo-PI fibres. This result reveals a decrease in the ordered structure along the fiber axis.

The orientation degree of crystals along the fiber axis is important in the final mechanical properties. The orientation factor (f_c) is determined according to Hermans' orientation function:

$$f_c = [3\langle \cos^2 \varphi_c \rangle - 1]/2 \quad (1)$$

where $\langle \cos^2 \varphi_c \rangle$ is the orientation parameter of the molecular chain axis (*c*) along the fiber axis, and it is determined according to the Wilchinsky model and crystal symmetry of the prepared PI fibers with characteristic reflections in the equatorial direction. For the reflection plane (*hkl*), the orientation parameter $\langle \cos^2 \varphi_c \rangle$ can be calculated by using Eq. (2):

$$\cos^2 \Phi_c = \frac{\int_0^{\pi} I(\Phi_c) \cos^2 \Phi_c \sin \Phi_c d\Phi_c}{\int_0^{\pi} I(\Phi_c) \sin \Phi_c d\Phi_c} \quad (2)$$

where Φ_c represents the angle between the fiber axis and the c axis of the crystal unit cell, and $I(\Phi_c)$ denotes the intensity along the reflection plane (hkl). Detailed results are listed in Table 4. Their orientation factors are 0.844, 0.857, 0.863, 0.876, 0.875, 0.869 and 0.873, which correspond to homo-PI-0, co-PI-1, co-PI-2, co-PI-3, co-PI-4, co-PI-5 and homo-PI-0' fibers, respectively. It can be found that the orientation factor of all PI fibers is higher than 0.80, which indicates that the crystalline molecular chains possess a highly ordered structure along the fiber axis. Nevertheless, among all fibers, the homo-PI-0 fiber displays the lowest f_c of 0.844, which is possibly due to the lowest draw ratio of 1.2 n (Table 1). Definitely, a high draw ratio facilitates the easy orientation of the molecular chains orient to form an ordered structure. However, the orientation degree of co-PI fibers only exhibits minimal difference.

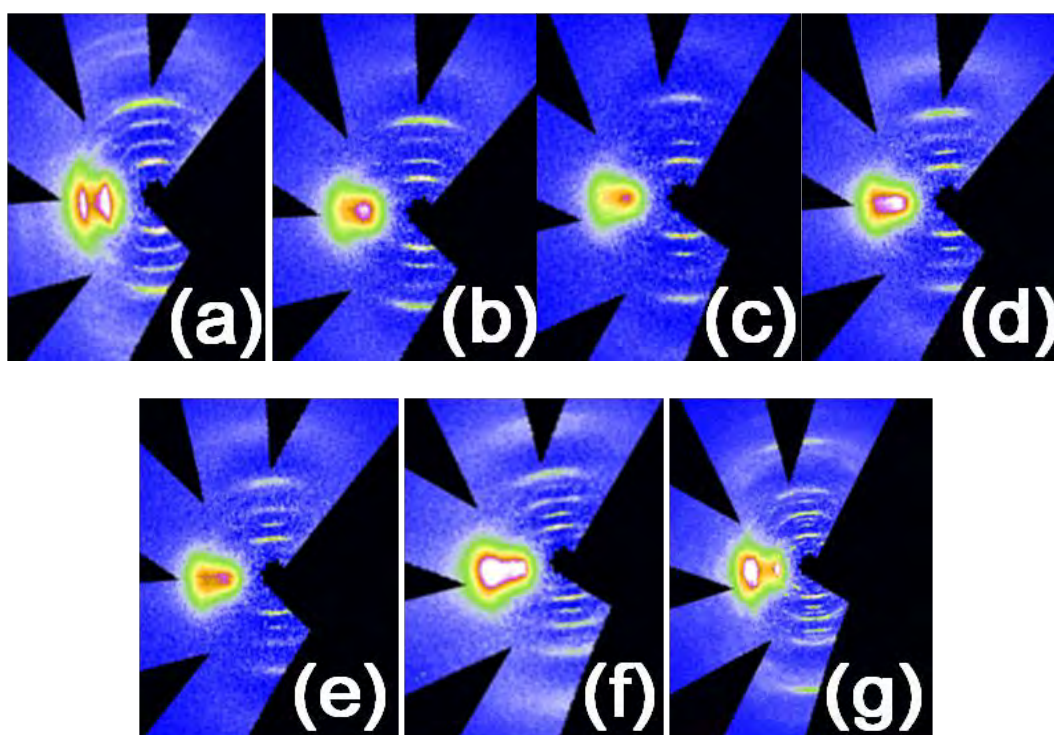


Fig. 5. 2D WAXD patterns of the prepared fibers with different diamine monomer molar ratios: (a) homo-PI-0, (b) co-PI-1, (c) co-PI-2, (d) co-PI-3, (e) co-PI-4, (f) co-PI-5, and (g) homo-PI-0'.

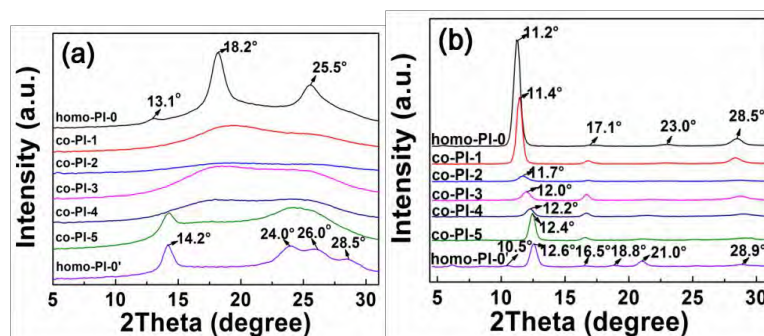


Fig. 6. 1D WAXD patterns of the prepared fibers with different diamine monomer molar ratios: (a) equator direction, (b) meridian direction.

Table 4. Crystallinity, orientation factor and microvoid parameters of the prepared PI fibers with different diamine monomer molar ratios.

Sample	WAXD	SAXS								\bar{R} (Å)
	Orientation factor, f_c	L (nm)	B_ϕ (°)	R_1 (Å)	R_2 (Å)	R_3 (Å)	ω_1 (%)	ω_2 (%)	ω_3 (%)	
homo-PI-0	0.844	480	3.60	32.5	111.8	211.3	36.2	23.9	39.9	122.8
co-PI-1	0.857	463	2.34	51.2	105.4	171.1	26.5	31.3	41.2	118.1
co-PI-2	0.863	456	2.59	45.2	90.7	177.4	27.2	29.8	43.0	115.6
co-PI-3	0.876	423	3.43	33.4	98.9	182.8	45.1	23.5	31.4	95.7
co-PI-4	0.875	487	3.12	51.9	102.0	167.0	31.0	33.1	35.9	109.9
co-PI-5	0.869	489	3.66	39.9	90.1	168.4	25.2	27.7	47.1	114.3
homo-PI-0'	0.873	483	3.41	36.7	99.2	190.7	25.7	32.9	41.4	121.0

3.5 Microvoid morphology

In addition to the crystallinity and molecular orientation, the porous structure of polymeric fibers also influences the mechanical properties. The microvoids in fibers prepared by the two-step method are formed during the dual-diffusion and thermal-imidization processes. As reported in literature [23-25], when the sample-to-detector distance reaches to a certain length, a sharp and elongated streak in 2D SAXS patterns comes from the oriented needle-shaped scattering moieties. Fig.7 shows that a sharp and elongated streak along the equatorial direction can be observed in homo-PI and co-PI fibers. The streak is mainly associated with the long and narrow microvoids that are preferably aligned parallel to the fiber axis direction.

To calculate the dimension (average length and radius) of microvoids in fiber, as illustrated in Fig. 12, the Ruland formula in Eq. (3) can be applied to calculate the average length of microvoids parallel to the fiber axis:

$$B_{obs} = \frac{2\pi}{Lq} + B_\phi \quad (3)$$

where B_{obs} , L , and B_ϕ denote the integral breadth, average length and misorientation of microvoids, respectively, and q represents the scattering vector.

The Guinier function in Eq. (4) is used to calculate the radius of microvoids in the cross-section:

$$I(q) = I(0) \exp\left(\frac{-q^2 R^2}{5}\right) \quad (4)$$

where R is the radius of microvoids in the cross-section, $I(0)$ represents the incident intensity, and $I(q)$ denotes the scattering intensity.

When the Fankuchen successive tangent method is applied, the average radius of microvoids is calculated according to Eq. (5) :

$$\bar{R} = \sum R_i \omega_i \quad (i = 1, 2, 3 \text{ t}) \quad (5)$$

where \bar{R} is the average radius of microvoids, R_i and ω_i are the radius of different sizes and the corresponding volume percentage of microvoids. Detailed results are listed in Table 4. The misorientation of microvoids (\bar{R}) of all fibers is less than 3.7° , which indicates the preferably orientation of microvoids along the fiber axis. The average lengths of microvoids are 480, 463, 456, 423, 487, 489 and 483 nm, and the average radii are 122.8, 118.1, 115.6, 95.7, 109.9, 114.3 and 121.0 Å, for homo-PI-0, co-PI-1, co-PI-2, co-PI-3, co-PI-4, co-PI-5 and homo-PI-0' fibers, respectively. The average length and radius of microvoids decrease with the increase in *p*-mHBOA content from 10% to 50%. When the *p*-mHBOA content increases continuously, the average length and radius of microvoids increase to 498 nm and 114.3 Å, respectively. It should be mentioned that the co-PI-3 displays the shortest average length (L) and the smallest average radius (\bar{R}) of microvoids in all PI fibers.

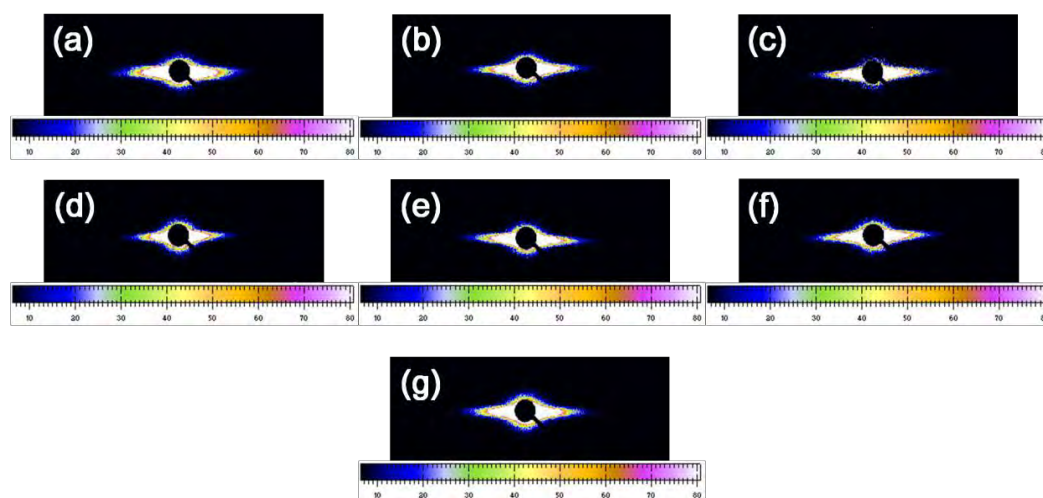


Fig. 7. 2D SAXS patterns of the prepared fibers with different diamine monomer molar ratios: (a) homo-PI-0, (b) co-PI-1, (c) co-PI-2, (d) co-PI-3, (e) co-PI-4, (f) co-PI-5, and (g) homo-PI-0'.

3.6 Mechanical properties

Mechanical property is considered a significant parameter for synthetic fibers, especially in engineering applications. Fig. 8 illustrates the variation of the mechanical properties with *p*-mHBOA content, and detailed information is listed in Table 5. Evidently, homo-PI-0 and homo-PI-0' fibers possess the fracture strengths of 8.33 cN/dtex and 26.67 cN/dtex, and initial moduli of 592.97 cN/dtex and 811.79 cN/dtex, respectively. From co-PI-1 to co-PI-5, their tensile strengths are 16.80 cN/dtex, 23.24 cN/dtex, 30.31 cN/dtex, 29.19 cN/dtex and 27.79 cN/dtex, and initial moduli are 794.64 cN/dtex, 877.64 cN/dtex, 894.88 cN/dtex, 873.46 cN/dtex and 828.94 cN/dtex, respectively. Elongation at break gradually increases from 1.48% to 3.42% with *p*-mHBOA content. The *p*-mHBOA content increases from 10% to 50%, and the fracture strength and initial modulus increase gradually. Particularly, the co-PI-3 fiber (50% *p*-mHBOA) exhibits the highest fracture strength (30.31 cN/dtex) and initial modulus (894.88 cN/dtex). However, a further increase in *p*-mHBOA content decreases the fracture strength and initial modulus.

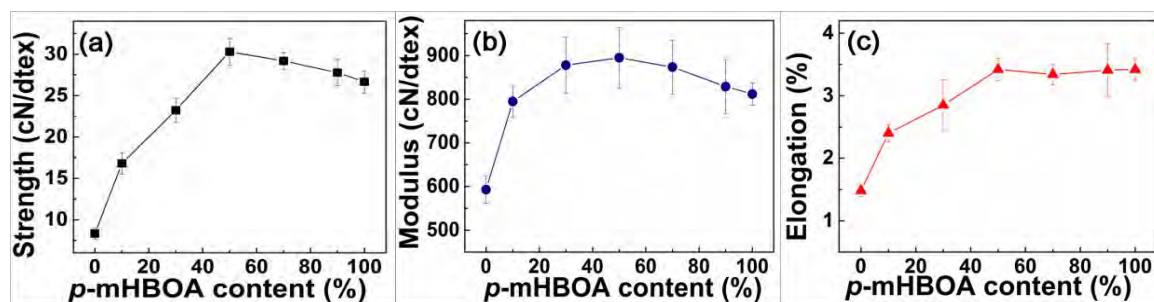


Fig. 8. Variation of mechanical properties with *p*-mHBOA content for the prepared PI fibers.

Table 5 Mechanical properties of the PI fibers.

Sample	<i>p</i> -mHBOA/ <i>p</i> -PDA		Draft ratio /draw ratio	Mechanical properties		
	(molar ratio)			Strength (cN/dtex)	Modulus (cN/dtex)	Elongation (%)
homo-PI-0	0/10		3.0/1.2	8.33±0.67	592.97±30.92	1.48±0.09
co-PI-1	1/9		3.0/1.5	16.80±1.29	794.64±35.75	2.40±0.14
co-PI-2	3/7		3.0/1.5	23.24±1.45	877.94±64.08	2.85±0.41
co-PI-3	5/5		3.0/1.5	30.31±1.63	894.88±68.47	3.42±0.18
co-PI-4	7/3		3.0/1.5	29.19±1.03	873.46±61.88	3.34±0.16
co-PI-5	9/1		3.0/1.5	27.79±1.57	828.94±61.75	3.41±0.42
homo-PI-0'	10/0		3.0/1.5	26.67±1.35	711.79±25.53	3.42±0.17

The density of the co-PI-3 fiber is determined at 1.479 g cm⁻³ through the Archimedean principle using a water bath attached to a microbalance. Hence, the fracture strength and initial modulus of the co-PI-3 fiber are 4.40 GPa and 129.8 GPa, respectively. In comparison with PI fibers reported in previous literatures, the co-PI-3 fiber possesses the highest fracture strength.

4. CONCLUSIONS

A series of high performance polyimide copolymer fibers are successfully prepared based on the copolymerization of BPDA, *p*-PDA and *p*-mHBOA via the traditional two-step method. As-prepared PI fibers show the T_g s in the range of 290 °C–325 °C, and $T_{5\%}$ values within 557 °C–593 °C and 528 °C–542 °C in nitrogen and air atmospheres, respectively, which indicate excellent thermal and thermo-oxidative stability. Deconvoluted FTIR results suggest that copolymerization is conducive to enhancing the intermolecular H-bonding, and the intramolecular H-bonding gradually increases with increasing *p*-mHBOA content. The ordered molecular packing along the transversal direction of fibers is damaged by the copolymerization, and the co-PI-3 with the *p*-mHBOA/*p*-PDA molar ratio of 5/5 presents the lowest crystallinity (only 9.3%). Nonetheless, the crystal orientation of co-PI fibers is higher than that of homo-BPDA/*p*-PDA fiber, and the copolymerization is beneficial to reduce the dimension of the microvoids in fibers. The optimal mechanical properties of co-PI fibers are obtained when the *p*-mHBOA/*p*-PDA molar ratio is 5/5. The fracture strength and initial modulus are 30.31

cN/dtex (4.40 Gpa) and 894.88 cN/dtex (129.8 Gpa), respectively. These results indicate that a strong intermolecular interaction, high crystal orientation and minimal defect contribute to the development of high fracture strength and initial modulus.

Acknowledgments

The authors are grateful to the financial supports from National Basic Research Program of China (2014CB643603) and National Key R&D Program of China (2017YFB0308300).

References

- [1] L. Li, C. Guan, A. Zhang, D. Chen, Z. Qing, Thermal stabilities and the thermal degradation kinetics of polyimides, *Polym. Degrad. Stab.* 84(3) (2004) 369–373.
- [2] F. Li, L. Huang, Y. Shi, X. Jin, Z. Wu, Z. Shen, K. Chuang, R.E. Lyon, F.W. Harris, S.Z.D. Cheng, Thermal degradation mechanism and thermal mechanical properties of two high-performance aromatic polyimide fibers, *J. Macromol. Sci., Part B: Phys.* 38(1-2) (2006) 107–122.
- [3] Y. Zhao, T. Feng, G. Li, F. Liu, X. Dai, Z. Dong, X. Qiu, Synthesis and properties of novel polyimide fibers containing phosphorus groups in the main chain, *RSC Adv.* 6(48) (2016) 42482–42494.
- [4] Y. Zhao, G. Li, F. Liu, X. Dai, Z. Dong, X. Qiu, Synthesis and properties of novel polyimide fibers containing phosphorus groups in the side chain (DATPPO), *Chin. J. Polym. Sci.* 35(3) (2017) 372–385.
- [5] J. Dong, C. Yang, Y. Cheng, T. Wu, X. Zhao, Q. Zhang, Facile method for fabricating low dielectric constant polyimide fibers with hyperbranched polysiloxane, *J. Mater. Chem. C* 5(11) (2017) 2818–2825.
- [6] W.E. Dorogy Jr, A.K.S. Clair, Low dielectric polyimide fibers, *US Pat.*, 5,367,046, 1994.
- [7] K. Bohnert, P. Gabus, J. Kostovic, H. Brändle, Optical fiber sensors for the electric power industry, *Opt. Las. Eng.* 43(3) (2005) 511–526.
- [8] Y. Zhao, Z. Dong, G. Li, X. Dai, F. Liu, X. Ma, X. Qiu, Atomic oxygen resistance of polyimide fibers with phosphorus-containing side chains, *RSC Adv.* 7(9) (2017) 5437–5444.
- [9] H. Niu, M. Huang, S. Qi, E. Han, G. Tian, X. Wang, D. Wu, High-performance copolyimide fibers containing quinazolinone moiety: Preparation, structure and properties, *Polymer* 54(6) (2013) 1700–1708.
- [10] C. Yin, J. Dong, D. Zhang, J. Lin, Q. Zhang, Enhanced mechanical and hydrophobic properties of polyimide fibers containing benzimidazole and benzoxazole units, *Eur. Polym. J.* 67 (2015) 88–98.
- [11] L. Penn, F. Larsen, Physicochemical properties of kevlar 49 fiber, *J. Appl. Polym. Sci.* 23(1) (1979) 59–73.
- [12] H. Yang, *Kevlar aramid fiber*, Wiley: Chichester, UK, 1993.
- [13] N.N. Machalaba, K.E. Perepelkin, Heterocyclic aramide fibers-production principles, properties and application, *J. Ind. Text.* 31(3) (2002) 189–204.
- [14] D.J. Sikkema, Design, synthesis and properties of a novel rigid rod polymer, PIPD or M5': high modulus and tenacity fibres with substantial compressive strength, *Polymer* 39(24) (1998) 5981–5986.
- [15] M. Afshari, D.J. Sikkema, K. Lee, M. Bogle, High performance fibers based on rigid and flexible polymers, *Polym. Rev.* 48(2) (2008) 230–274.
- [16] H. Niu, S. Qi, E. Han, G. Tian, X. Wang, D. Wu, Fabrication of high-performance copolyimide fibers from 3,3',4,4'-biphenyltetracarboxylic dianhydride, *p*-phenylenediamine and 2-(4-aminophenyl)-6-amino-4(3H)-quinazolinone, *Mater. Lett.* 89 (2012) 63–65.
- [17] M. Lammers, E. Klop, M. Northolt, D. Sikkema, Mechanical properties and structural transitions in the new rigid-rod polymer fibre PIPD (M5') during the manufacturing process, *Polymer* 39(24) (1998) 5999–6005.

- [18] T. Zhang, J. Jin, S. Yang, G. Li, J. Jiang, A rigid-rod dihydroxy poly (*p*-phenylene benzobisoxazole) fiber with improved compressive strength, *Carbohydr. Polym.* 78(2) (2009) 364–366.
- [19] T. Zhang, J. Jin, S. Yang, G. Li, J. Jiang, Effect of hydrogen bonding on the compressive strength of dihydroxypoly (*p*-phenylenebenzobisoxazole) fibers, *ACS Appl. Mater. Interfaces* 1(10) (2009) 2123–2125.
- [20] C. Lin, J. Kuo, C. Chen, J. Fang, Investigation of bifurcated hydrogen bonds within the thermotropic liquid crystalline polyurethanes, *Polymer* 53(1) (2012) 254–258.
- [21] H. Dong, Z. Xin, X. Lu, Y. Lv, Effect of N-substituents on the surface characteristics and hydrogen bonding network of polybenzoxazines, *Polymer* 52(4) (2011) 1092–1101.
- [22] R. Snyder, B. Thomson, B. Bartges, D. Czerniawski, P. Painter, FTIR studies of polyimides: thermal curing, *Macromolecules* 22(11) (1989) 4166–4172.
- [23] Y. Lu, Y. Wang, R. Chen, J. Zhao, Z. Jiang, Y. Men, Cavitation in isotactic polypropylene at large strains during tensile deformation at elevated temperatures, *Macromolecules* 48(16) (2015) 5799–5806.
- [24] Y. Tang, Z. Jiang, Y. Men, L. An, H.F. Enderle, D. Lilge, S.V. Roth, R. Gehrke, J. Rieger, Uniaxial deformation of overstretched polyethylene: In-situ synchrotron small angle X-ray scattering study, *Polymer* 48(17) (2007) 5125–5132.
- [25] W. Ruland, Small-angle scattering studies on carbonized cellulose fibers, *J. Polym. Sci., Part C: Polym. Symp.* 28(1969) 143–151.